"Chevron" Local Layer Structure in Surface-Stabilized Ferroelectric Smectic-C Cells

T. P. Rieker,[1] N.A. Clark,[1] G. S. Smith,[1,2] D. S. Parmar,[1] E. B. Sirota,[2] and C. R. Safinya[2]

[1]Department of Physics, Condensed Matter Laboratory, and Center for Optoelectronic Computing Systems,
University of Colorado, Boulder, Colorado 80309

[2]Exxon Research and Engineering Company, Annandale, New Jersey 08801

High-resolution x-ray scattering studies of thin smectic-C (SmC) samples prepared between solid plates by cooling from the smectic-A phase reveal a surprising "chevron" structure of tilted layers. This structure is formed as a response to the shrinking of the SmC layers while anchored to the solid plates. The layer tilt is independent of surface treatment. Our results provide fundamental new information on the structure and surface interactions of SmC layers and provide evidence for a new SmC defect.

PACS numbers: 61.30.Gd, 61.30.Cz, 78.62.+i

In recent years, a great deal of study has been made of cells consisting of thin layers of chiral (ferroelectric) smectic-C (SmC) liquid crystal between solid plates. Such cells, when thin enough to exclude the bulk chiral SmC helix, exhibit high-speed, bistable electro-optical switching between orientation states stabilized by surface interactions.[1-3] These thin surface-stabilized SmC samples, both chiral and nonchiral, when viewed in a polarized-light microscope are striking in that they exhibit ubiquitous features which are not found in thicker SmC or other smectic preparations. Particularly prevalent are the so-called zigzag walls.[3,4] These defects consist of narrow walls running in a zigzag fashion nearly normal to the layers and broad walls running parallel to the layers. In thicker SmC cells ($h > 3$ μm) the zigzag walls separate regions of uniform but different optical contrast in polarized transmission microscopy. This observation led us to question the earlier assumption that the SmC layers were normal to the plates in surface-stabilized ferroelectric liquid-crystal cells (SSFLC)[1] and to suggest that zigzag walls separated regions of different tilt of the layers relative to the bounding plates.[3] This question of the equilibrium local layer structure (LLS) in thin SmC samples motivated the x-ray study which we report in this Letter.

The sample cells were prepared as shown in Fig. 1. The liquid crystal is the dielectric of thickness $h \simeq 3$ μm in a transparent capacitor formed by a pair of indium-tin oxide coated glass cover slips spaced by a 1-cm-diam polyimide ring. The glass thickness was minimized to keep x-ray attenuation and stray scattering at negligible levels. The cells were filled with either a commercial mixture[5] or DOBAMBC (p-decyloxybenzylidene-p'-amino-2-methylbutyl-cinnamate)[6] in the isotropic phase, then cooled into the smectic-A (SmA) and SmC phases. Uniform alignment of the director in the SmA phase was obtained either by anisotropic surface treatment[7] or by shearing. Cells were evaluated optically to ensure uniform alignment and that the bulk ferroelectric liquid-crystal director helix was suppressed. Surface treat-

ments tested were as follows: (1) nylon buffed with a brush with both parallel (same brushing direction on both plates) and antiparallel brushing (lozenges); (2) nylon buffed with a buffing wheel, parallel brushing (open circles, squares, triangles, and inverted triangles and filled squares and inverted triangles); (3) PVA buffed with a buffing wheel, parallel brushing (filled triangles); (4) an asymmetric cell with a brushed nylon surface and a surface coated with the surfactant hexamethyldisilizane (filled circles). The symbols refer to Fig. 3.

The LLS in these thin SmC preparations was probed via high-resolution x-ray scattering with a high-intensity source and computer-controlled Huber four-circle diffractometer. Experiments were performed at the Exxon Research and Engineering Co. Laboratory on an 18-kW rotating-anode x-ray generator (Rigaku model RU300) and at the Stanford Synchrotron Radiation Laboratory (SSRL), beam-line VII-2.[8] The x-ray scattering geometry is given in Fig. 1.

The cell was mounted on a goniometer with its midplane ($x = 0$) on the axis for rotation about y (Fig. 2). The cell was rotated about the y axis until the glass plates were normal to the incident wave vector $\mathbf{K}_i$ as determined by our shining a laser along the beam path and rotating the sample until the reflected laser beam re-
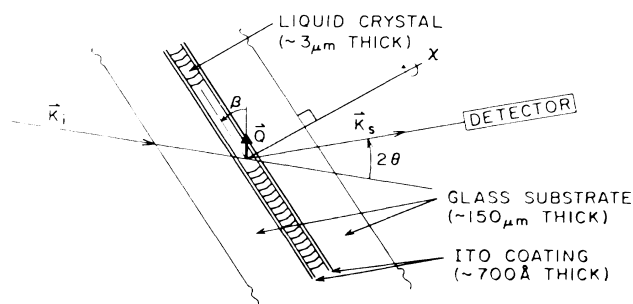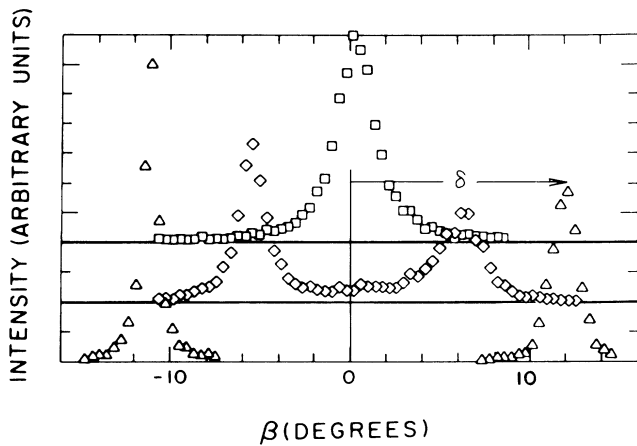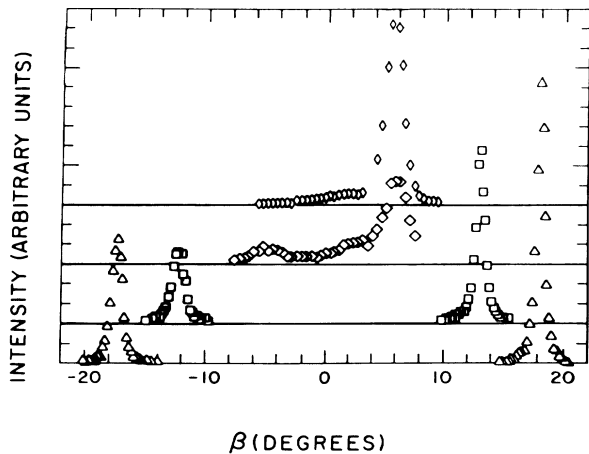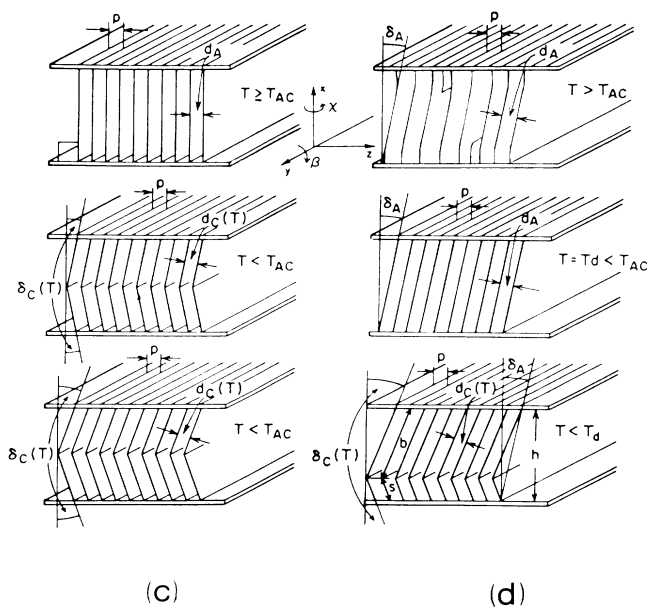

FIG. 1. The scattering geometry.

β(DEGREES)

(a)

β(DEGREES)

(b)

(c)   (d)

traced its path. This enabled us to orient the scattering vector $Q = K_s - K_i$ relative to the plane of the glass plates ($\beta = 0$ when Q is parallel to the plates). A two-stage oven was then placed over the cell providing temperature stability to ± 4 mK. The detector arm orientation (2θ) was then set to the approximate angle for smectic-layer Bragg diffraction. The sample was rotated about the normal to the cover glass planes (X in Fig. 1) to bring the rubbing direction and therefore the Bragg wave vectors into the scattering plane. Once this was achieved, 2θ and β were varied (at a set sample temperature) to locate the Bragg peaks. These values were then used to determine the smectic-layer spacing (d) and tilt angle (δ). Layer orientation data are presented as plots of scattered intensity $I(\beta)$ vs β.

Different regions of a given sample were studied to probe the variation of the structure with position. The area illuminated by the x-ray beam in the rotating-anode experiments was 1×3 mm^2, which typically covered many zigzag domains, including regions on both sides of zigzag walls. At SSRL the beam area was sufficiently small (100×200 μm) that the *homogeneously structured regions separated by the zigzag walls could be probed and the true LLS observed.* These areas were selected via polarized-light microscopy to show no visible defects.

Our experimental results are as follows:

(1) In the SmA phase the layers are tilted relative to the bounding-plate normal at an angle δ_A that depends on the sample history. Careful cooling through the isotropic-SmA transition generally produces SmA layers normal to the plates in the materials studied.

(2) In the SmC phase there are two LLS scenarios, one for $\delta_A = 0$ and the other for $\delta_A \neq 0$. Typical data for $\delta_A = 0$ are shown in Fig. 2(a). In the SmA phase a plot of scattered intensity $I(\beta)$ vs β shows a single peak at $\beta = 0$. As T decreases through the SmA-to-SmC transition this peak splits to form a pair of peaks, symmetrically located at $\pm \delta_C(T)$. The splitting increases monotonically with decreasing temperature to saturate at about $17\,°C$ in the mixture and $25\,°C$ in DOBAMBC. At

FIG. 2. (a),(b) Scattered intensity $I(\beta)$ vs β, the angle between the substrate planes and the x-ray scattering vector Q, from a 100×100-μm^2 zigzag defect-free area of a SSFLC cell. These plots indicate unambiguously that the LLS in our SSFLC cell has the layers planar, but with two distinct tilts in the SmC phase, with respect to the bounding plate normal. (a) $\delta_A = 0$ (SmA layers normal to the bounding plates). Squares, $T = T_c + 0.2\,°C$; lozenges, $T = T_c - 0.5\,°C$; triangles, $T = T_c - 2.2\,°C$. (b) $\delta_A = 7°$ (SmA layers tilted). Small lozenges, $T = T_c + 6.9\,°C$; large lozenges, $T = T_c - 0.5\,°C$; squares, $T = T_c - 3.1\,°C$; triangles, $T = T_c - 17.0\,°C$. (c) LLS scenario for $\delta_A = 0$, showing the formation of symmetric chevrons for $T < T_c$. (d) LLS scenario for $\delta_A > 0$, layer tilt and accompanying dislocations in the SmA phase, tilted layers with no dislocations at $T = T_d$, and the formation of the asymmetric chevron for $T < T_d$.
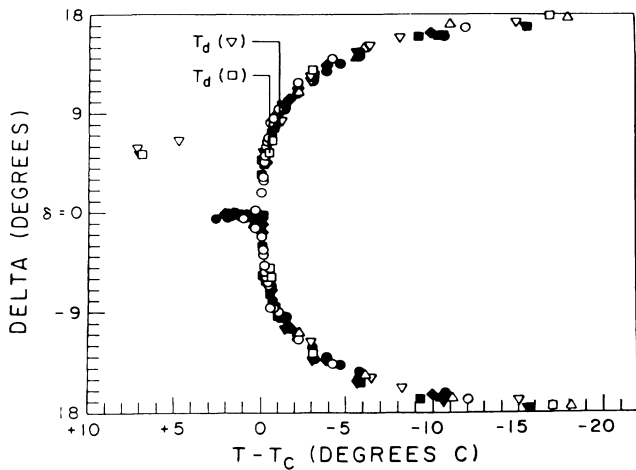
FIG. 3. Layer tilt δ as a function of $T - T_c$, as obtained from the peak location in $I(\beta)$ data, showing upper and lower branches located symmetrically about $\delta = 0$. (Solid points, rotating anode; open points, SSRL.) The data yield no distinction among the various surface treatments used (see text). With the exception of the open inverted triangle and open square data, the points lie on a common curve with $\delta \rightarrow 0$ as $T \rightarrow T_c$ and $\delta_A = 0$ in the SmA phase. For the open inverted triangles and open squares the SmA layers were tilted with $\delta_A \simeq 7°$ in both the SmA and SmC phases for $T > T_d = T_c - 1°C$, the temperature at which the peak on the lower branch appears with decreasing T. This and the fact that the open inverted triangle and open square data lie on the common curve for $T < T_d$ indicate the formation of the asymmetric chevron for $T < T_d$.
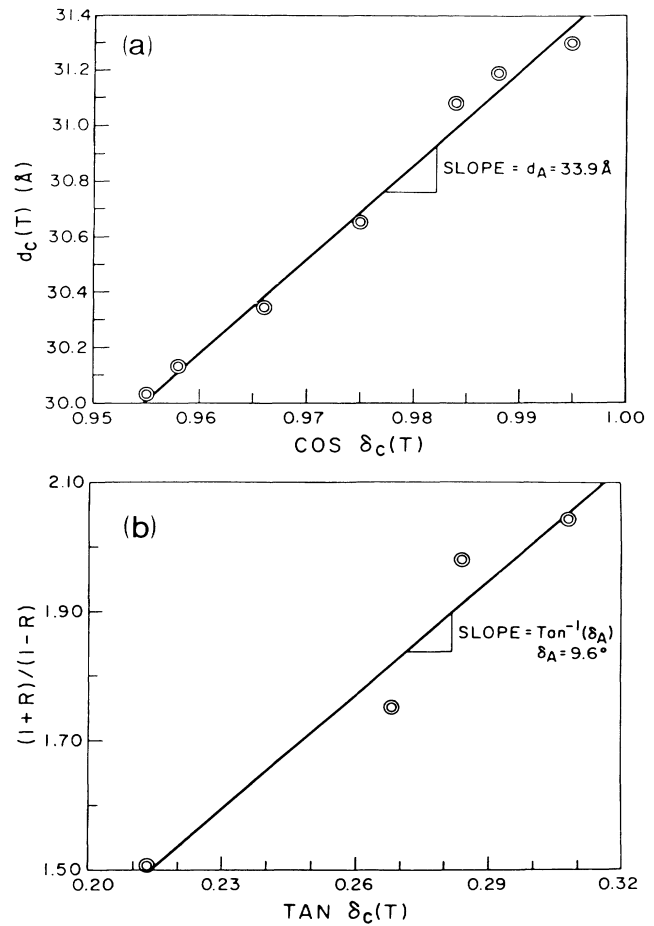

FIG. 4. (a) SmC layer spacing $d_C(T)$ vs $\cos\delta_C(T)$, the SmC layer tilt angle. The slope is $d_A = 33.9$ Å which compares well with the 2θ determined value of 31.4 Å. (b) $(1+R)/(1-R)$ vs $\tan\delta_C$, where $R = I_s/I_b$ is the intensity ratio of the two scattering peaks.

lower temperatures in the SmC phase the peaks in $I(\beta)$ become very sharp (full width at half height $d\beta \simeq 1.2$ degrees) and contain more than 85% of the scattering intensity, indicating a LLS of tilted higher planar layers in nearly equal amounts. $\delta_C(T)$ is a reversible equilibrium function, monotonically increasing with decreasing temperature, which, as shown in Fig. 3, is completely independent of surface treatment!

(3) In some cases, the two SmC peaks are of significantly different intensities, as shown in Fig. 2(b). In this case an increase in the temperature causes the smaller peak to get weaker and disappear at a temperature T_d in the SmC phase. For $T < T_d$ the peak positions $\delta_C(T)$ lie on the typical curve (open inverted triangles and open squares in Fig. 3). For $T > T_d$ the location of the surviving peak becomes independent of T, maintaining the value of $\delta_C(T_d)$ that it had at the disappearance of the small peak, right up into the SmA phase. This is the scenario for layers tilted in the SmA phase $[\delta_A = \delta_C(T_d)]$. It is also found to be reversible.

(4) The SmC layer tilt angle δ_C, determined from the peak location in $I(\beta)$, is related to the SmC layer spacing $d_C(T)$ and the SmA layer spacing d_A (both oriented from the location of the peak in 2θ) as follows [see Fig.

4(a)]:

$$d_C(T) = d_A[\cos\delta_C(T)]. \qquad (1)$$

(5) Electric fields of $E < 5$ V/μm applied to ferroelectric SmC samples had no effect on the layer tilt.

These experimental facts have led us to formulate the following anchored-layer model which accounts for all of the observed features of the LLS temperature dependence. We begin by noting that the observed SmC layer tilt angle $\delta_C(T)$ given by Eq. (1) is that which maintains the pitch of the layers, p, at its SmA value $p = d_A$, at all temperatures in the SmC phase [$p =$ length/layer in the z direction; see Fig. 2(c)]. This suggests that in order to maintain p, the layers tilt as a response to the shrinking ($d_C < d_A$) which occurs in the SmC phase. Figure 2(c) shows the SmA phase in which the layers have formed normal to the plates. We assumed that once the layers have formed and are anchored, the anchoring positions

are fixed, i.e., the intersections of the layers and the glass plates cannot move in the z direction. In this case the SmA layers are continuous: There is no need for dislocations. If we further assume that the layers remain continuous, i.e., dislocations do not form, then any LLS must have $p = d_A$. The only SmC-phase LLS having $p = d_A$ is that having a uniform tilt according to Eq. (1). Finally, the only kind of tilt which preserves the anchoring condition is the symmetric chevron.

Now consider that the layers form with a tilt δ_A in the SmA phase. At the surface the layers are normal to the bounding plates because of the director alignment parallel to z imposed by the bounding surface and so at the surface $p_s = d_A$. In the middle $p_m = d_A \cos\delta_A$ so that dislocations must be present to make up for $p_s \neq p_m$, as discussed by Williams and Kleman[9] and shown in Fig. 2(d). As the sample is cooled through the SmA-to-SmC transition the layers begin to shrink and these dislocations move toward the sample center, reaching the center and completing whole layers when $\delta_C(T) = \delta_A$, i.e., when the SmC pitch decreases to $p = d_A$. At this point further shrinkage of the SmC layers is accommodated by tilting of the layers through the angle $\delta_C(T)$ and chevron formation. However, now the chevron is asymmetric, with the sharp break in the layers initially forming at one surface and moving toward the middle as T decreases. If R gives the ratio of the lengths of the chevron sides ($R = s/b$), then, with reference to Fig. 2(d), the geometry gives

$$(1+R)/(1-R) = \tan\delta_C/\tan\delta_A. \qquad (2)$$

Using the integrated intensities of the small to big peak $R = I_s/I_b$ to measure R, we plot the data in Fig. 4(b) from the $I(\beta)$'s in Fig. 2(d). The fitted slope $\tan\delta_A - 1$ gives $\delta_A = 9.6°$ which agrees favorably with the directly measured value of 7.2°. This scenario thus accounts for the behavior when the two peaks in $I(\beta)$ are unequal in intensity, and indicates that for the surface treatments used here the molecules are parallel to the plates in the SmA phase.

We have demonstrated that the LLS in a thin SmC slab prepared between solid plates with planar boundary conditions is chevronlike, with the layers tilted relative to the plates and making an abrupt reorientation at a planar interface parallel to the bounding planes. This reorientation is a new kind of liquid-crystal defect, the first observed of the class of planar liquid-crystal defects. Appreciation of this chevron structure has enabled us to understand a variety of features of SSFLC cells, including the full three-dimensional structure of zigzag walls and the director fields.[10]

[1]N. A. Clark and S. T. Lagerwall, Appl. Phys. Lett. **36**, 899 (1980).

[2]N. A. Clark and S. T. Lagerwall, Ferroelectrics **59**, 25 (1984).

[3]M. A. Handschy and N. A. Clark, Ferroelectrics **59**, 69 (1984).

[4]Y. Ouchi, H. Takezoe, and A. Fukuda, Jpn. J. Appl. Phys. Pt. 1 **26**, 1 (1987).

[5]C2C10 is 4'-[(s)-2-methyl-3-oxa-1-pentyloxy]phenyl 4-(decyloxy)benzoate, $C_{10}H_{21}-O-Ph-COO-Ph-O-CH_2-CH(CH_3)-(OC_2H_5)$. 10.O7* is 4'[(s)-1-hexyloxy-4-methyl]phenyl 4-(decyloxy)benzoate, $C_{10}H_{21}-O-Ph-COO-Ph-O-CH_2-CH_2-CH_2-CH(CH_3)-(C_2H_5)$. Obtained from Displaytech, Inc. Boulder, CO. The 50:50 mixture employed exhibits the following phases: $X < 0° < SmC < 50.5° < SmA < 62° < I$.

[6]R. B. Meyer, L. Liebert, L. Strzelecki, and P. Keller, J. Phys. Lett. **36**, L69–71 (1975).

[7]J. Cognard, Mol. Cryst. Liq. Cryst., Suppl. Ser. **1**, 1 (1982).

[8]D. E. Moncton and G. E. Brown, Nucl. Instrum. Methods Phys. Res. **208**, 579 (1983).

[9]C. E. Williams and M. Kleman, J. Phys. (Paris) Lett. **35**, L33 (1974).

[10]N. A. Clark, T. P. Rieker, G. S. Smith, and C. R. Safinya, to be published.